Published in final edited form as:
Mol Ther. 2005 February ; 11(2): 294–299. doi:10.1016/j.ymthe.2004.10.005.

BMP Gene Delivery for Alveolar Bone Engineering at Dental Implant Defects

Courtney A. Dunn[1,*], **Qiming Jin**[2,*], **Mario Taba Jr.**[2], **Renny T. Franceschi**[2,3], **R. Bruce Rutherford**[4], and **William V. Giannobile**[2,5,†]

1*Department of Orthodontics and Pediatric Dentistry, College of Engineering, University of Michigan, Ann Arbor, MI 48109, USA*

2*Department of Periodontics/Prevention/Geriatrics and Center for Craniofacial Regeneration, School of Dentistry, College of Engineering, University of Michigan, Ann Arbor, MI 48109, USA*

3*Department of Biological Chemistry, College of Engineering, University of Michigan, Ann Arbor, MI 48109, USA*

4*Ivoclar Vivadent-Dentigenix, Inc., Seattle, WA 98103, USA*

5*Department of Biomedical Engineering, College of Engineering, University of Michigan, Ann Arbor, MI 48109, USA*

Abstract

A challenge in the tissue engineering of alveolar bone surrounding oral or dental implants is achieving the targeted and sustained delivery of growth-promoting molecules at the osteotomy site. Bone morphogenetic protein-7 (BMP-7) has demonstrated the ability to stimulate bone regeneration in multiple skeletal sites, including the craniofacial complex. This study evaluates *in vivo* gene delivery of BMP-7 for bone tissue engineering around titanium dental implants. The maxillary first molar teeth of 44 Sprague–Dawley rats were extracted and allowed to heal for a period of 1 month. Large osteotomy defects were created in the edentulous ridge areas followed by the placement of dental implant fixtures. Recombinant adenoviral vectors encoding either the BMP-7 or the luciferase gene were delivered to the osseous defects using a collagen matrix. The kinetics of the gene expression was measured using *in vivo* bioluminescence optical imaging, while bone regeneration was evaluated under light and scanning electron microscopy. The results revealed sustained, targeted transgene expression for up to 10 days at the osteotomy sites with nearly undetectable levels by 35 days. Treatment of dental implant fixtures with Ad/BMP-7 resulted in enhancement of alveolar bone defect fill, coronal new bone formation, and new bone-to-implant contact. *In vivo* gene therapy of BMP-7 offers potential for alveolar bone engineering applications.

Keywords

gene therapy; osseointegration; bone morphogenetic proteins; gene transfer; biomimetics; tissue engineering

*These authors contributed equally to this work.
†To whom correspondence and reprint requests should be addressed at the Department of Periodontics, Prevention and Geriatrics, University of Michigan, 1011 N. University Avenue, Ann Arbor, MI 48109-1078, USA. Fax: +1 (734) 763 5503. E-mail: wgiannob@umich.edu.

Introduction

Tooth loss, often a consequence of trauma or disease, can lead to the destruction of nearly half of the original tooth-supporting (or alveolar) bone [1]. Traditional techniques for enhancing bone formation for dental implant placement include bone autografts, allografts, or guided bone regeneration [2]. These techniques, however, lack predictability in terms of new bone regeneration volume. Tissue engineering of alveolar bone using gene therapeutic approaches may offer potential for optimizing the delivery of growth-promoting molecules such as bone morphogenetic proteins (BMPs) at implant osteotomy sites [3,4].

BMPs are members of the TGF-β superfamily that are powerful regulators of cartilage and bone formation during embryonic development and regeneration in postnatal life [5]. Some BMPs also participate in the development and repair of extraskeletal tissues and organs such as the brain, kidney, and nerves [6]. Recent studies have demonstrated the expression of BMPs during tooth development and periodontal repair [7-9]. Bone morphogenetic protein-7 (BMP-7), also known as osteogenic protein-1, is a multifunctional member of the BMP family with multiple effects on bone formation and regeneration. BMP-7 stimulates bone regeneration around teeth [10], around endosseous dental implants [11], and in maxillary sinus floor augmentation procedures [12]. Although encouraging, results from these studies demonstrate partial regeneration and thus suggest a need for the development of improved methods of growth factor delivery.

In this study we demonstrate the sustained and targeted delivery of BMP-7 to large alveolar bone defects associated with dental implant fixtures. Bone regeneration of the defects was enhanced by the targeted gene transfer of BMP-7 at dental implant osteotomy sites.

Results

In Vivo Transgene Transduction Efficiency and Targeting

To determine the ability of BMP gene delivery to promote bone formation *in vivo*, we delivered gene therapy vectors to large implant osteotomy defects coincident with dental implant placement. The experimental model of extraction socket healing, implant osteotomy creation, and installation is shown in Figs. 1A and 1B. To evaluate the magnitude and targeting of gene delivery, we subjected the titanium dental implant fixtures to *in vivo* bioluminescence using optical imaging. All implants showed the targeted and sustained release of the gene product for a range of 10 to 35 days. All implants displayed the localized nature of expression in the near vicinity of the oral implants (Figs. 1C and 1D). The gene product was expressed strongly for the first few days with peak expression at day 4, then it steadily declined until it was nearly undetectable by 2–5 weeks. In one animal, some low-level luciferase expression [<1.25 relative light units (RLU)] was detected in the liver for up to 7 days post-gene delivery (data not shown).

BMP-7 Gene Delivery Promotes Bone Tissue Engineering *in Vivo*

We took block biopsies at 3, 7, 10, 14, and 28 days post-gene delivery and implant placement for descriptive histology and histomorphometric analysis. At 14 days post-surgery and gene delivery, early bone formation was seen along the defect borders. Several of the Ad/BMP-7-treated defects displayed tissue consistent with early osteoid formation throughout the defect area (Fig. 2). The Ad/Luc group exhibited normal bone healing, with most specimens showing minimal bone formation at the defect borders.

At 28 days post-gene transfer, bone formation was heightened both at the defect margins and along the dental implant surface in the Ad/BMP-7-treated sites (Fig. 2). In addition, the BMP-7-treated implants revealed a more mature lamellar bone formation, while Ad/Luc-treated defects contained mostly immature woven bone. We noted lamellar compaction and new bone in

BMP-7-treated defects beyond the calcein bone label landmark (Fig. 3). In addition, osseointegration as shown by SEM could be clearly seen (Fig. 3D).

Histomorphometric Analysis

The histomorphometric analysis of Ad/Luc and Ad/BMP-7 specimens 28 days after surgery is shown in Fig. 4. There was no significant difference in initial defect size between the groups ($P > 0.05$). The Ad/BMP treatment significantly increased the percentage bone defect fill in the defects by 50% ($P < 0.05$) compared to the Ad/Luc-treated group. The Ad/BMP-7 treatment also tended to enhance both coronal new bone formation (greater than twofold compared to the Ad/Luc group) and new bone-to-implant contact (by 50% compared to Ad/Luc). However, these differences were not statistically significant.

Discussion

A variety of techniques are used clinically to tissue engineer alveolar bone prior to or at the time of dental implant installation, such as osseous grafts and guided bone regeneration. However, limitations exist with these reconstructive approaches including lack of predictability and ability to achieve volumetric bone changes beyond the “envelope” of the alveolus. Advances in the field of tissue engineering and biomimetics offer significant potential to regenerate craniofacial structures using biologic mediators and matrices that mimic the tissue's original formative processes [13,14]. In this study, *in vivo* gene therapy was used to deliver BMP-7 to promote osteogenesis and osseointegration. The results demonstrated that *in vivo* gene transfer promotes bone regeneration around oral implants.

We utilized an adenoviral vector with a collagen matrix to immobilize the transgene at the dental implant defect site. Our previous experiments used dose ranges of 2–200 m.o.i. and the dose level chosen here led to optimal effects in both transduction efficiency and bone repair [15]. In addition, previous studies using adenovirus in collagen carriers for bone repair (i.e., periodontal wounds) used a similar dosing [16]. However, future dose levels using direct gene delivery of BMPs need to be explored. We recently demonstrated that this technique efficiently delivers platelet-derived growth factor genes to tooth-supporting structures [16]. Peak gene expression was found 1–7 days after delivery, with a subsequent decrease in expression over time (Figs. 1C and 1D). A low level of transgene expression was detected for up to 10–35 days, suggesting that the collagen was capable of immobilizing the virus for extended periods of time [16,17].

Efficient bone formation is essential for successful oral implant placement. There are many actions that BMPs exert to stimulate bone formation, including enhancing osteoblast proliferation and differentiation, acting as mitogens for undifferentiated cells, serving as chemoattractants for mesenchymal cells, and binding to type IV collagen [3,18,19]. It has been shown that topical administration of recombinant BMP-7 stimulates long bone union in large segmental bone defects [20].

Ad/BMP-7 transduction of human gingival fibroblasts repairs critical size cranial defects in a rat model [21]. Although adenovirus is an efficient means of gene transfer, it also elicits a significant immune response mediated by cytotoxic T cells [22]. The *ex vivo* approach may circumvent some of these problems by providing a more robust osteogenic response, although it requires two surgical procedures (for biopsy harvest and transplantation). Using this technique, critical size bony defects have been repaired completely with new bone [15,21,23, 24], as well as craniofacial defects compromised by postoperative radiotherapy [25].

Recent studies utilized *in vivo* gene delivery of BMPs to form bone ectopically in immunocompetent [26-29] and immunocompromised animals [28,29]. In immunocompetent

animals, ectopic bone formation was minimal and noted only after 3 weeks and the quantity and quality of bone were inferior to those of the immunosuppressed groups [28]. In some studies, animals with intact immune systems showed no bone formation and the suppressed groups did not show signs of osteogenesis until days 14–21 [29]. All groups suggested that the rapid immune response to the viral proteins decreased the expression of the gene in immunocompetent animals. Strategies to circumvent these problems ranged from immunosuppression to the use of AAV (adeno-associated virus) and gutted vectors from which viral coat protein genes have been deleted [26,29,30].

In this study, we achieved greater bone formation at implant defects when Ad/BMP-7 was used in immunocompetent animals. Other studies using AAV vectors for gene delivery of bone morphogenetic proteins without immunosuppression found impressive results [31,32]. New bone formation was initiated at 3 weeks, and expression of the protein was noted for 8 weeks [31,32]. These studies used *ex vivo* gene delivery to muscle-derived stem cells instead of osteoblastic cells, which are known to display different responses [26,30]. The use of AAV has the advantage of the minimal elicitation of an immune response. However, the longer term gene expression profile may prove a shortcoming once bone healing has completed.

In conclusion, the results from this study demonstrate that adenovirus delivered in a collagen matrix is capable of the targeted and sustained release of a transgene for up to 10 days at dental implant osteotomy sites. *In vivo* gene therapy of BMP-7 successfully initiated bone formation in bony defects surrounding oral implants. BMP-7 gene therapy offers potential for alveolar bone engineering applications.

Materials and Methods

Animals

A total of 44 10-week old Sprague–Dawley rats (approximate weight 250–300 g) were utilized in this study. Three of these animals were used for *in vivo* bioluminescence imaging. The animals were evaluated at 3, 7, 10, 14, and 28 days after gene therapy. Four animals each were evaluated at days 3, 7, and 10 and 15 animals were assigned to Ad/BMP-7 treatment and 15 animals served as controls with the Ad/Luc treatment for evaluation at 14 and 28 days. Five animals each were evaluated at 14 days and the remaining 10 were assayed at 28 days. All procedures were approved by the University of Michigan Committee of Use and Care of Animals. Animals were anesthetized under general anesthesia with ketamine (50 mg/kg) and xylazine (10 mg/kg). All procedures were performed using a surgical light microscope at 10× magnification (Aus Jena OPM 212T, Jena, Germany).

Tooth extraction, defect creation, implant placement, and gene delivery

The maxillary first molar teeth (M1) were extracted using an atraumatic technique. Full-thickness mucoperiosteal flaps were elevated around the teeth (M1) and then the crowns were sectioned into mesial and distal segments using a fissure bur under high-speed instrumentation. The root segments then were luxated with a spoon excavator and removed with an explorer and cotton forceps. The extraction sockets and soft tissues were allowed to heal for approximately 30 days.

After healing, a 1-cm incision was made that extended from M2 in the buccal vestibule area and extended beyond the M1 extraction site. A full thickness, mucoperiosteal flap was elevated and the alveolar ridge was exposed. The osteotomy sites were prepared by rotary instrumentation at 500 rpm with sterile saline irrigation using a 0.9-mm twist drill (Institut Straumann AG, Waldenburg, Switzerland). The osteotomy sites achieved a final length of 2 mm (Figs. 1A and 1B). A well-type defect then was prepared to half the depth of the implant

osteotomy with a No. 6 round carbide bur. Irrigation with sterile saline was utilized during osteotomy and defect creation.

Custom-fabricated, sterile, commercially pure, solid-cylinder titanium implants with a titanium plasma-sprayed surface were designed (Institut Straumann AG) to the appropriate dimensions for placement into the rat maxilla (2 mm in length and 1 mm in diameter). The implants were press fit into position and evaluated for primary stability. The remaining surface of the implants and the osseous defects received treatment with approximately 10 μl of a 2.6% collagen gel (Matrix Pharmaceutical, Fremont, CA, USA) containing 2.5×10^{11} particles of either Ad/Luc (kindly donated by Selective Genetics, Inc., San Diego, CA, USA) or Ad2/BMP-7 [21] (Fig. 1). Both of these recombinant adenoviruses are driven by the CMV promoter. The particle-to-pfu ratio was 120:1. The surgical field was closed by means of tissue glue (PeriAcryl, *n*-butyl cyanoacrylate; GluStitch, Inc., Delta, BC, Canada). The animals were observed postoperatively on a heating pad until fully alert to ascertain their response to surgery. They were closely monitored for complications including pain, discomfort, and infection. A bone fluorochrome was administered 1 day after surgery [im injection of calcein (3,3′-bis-*N*,*N*-di(carboxymethyl) aminomethylfluorescein), 10 mg/kg] to demarcate the region between old and new bone formation [33]. Our early pilot experiments (data not shown) have revealed that the defect model leads to complete healing in some of the animals under normal circumstances (without gene transfer by days 35–49). To maintain energy and prevent infection, animals were given a 10% dextrose solution containing 268 μg/L ampicillin for 1 week postsurgery.

In vivo transgene transduction efficiency and targeting

To evaluate the efficiency and to localize gene expression around the implant surfaces, implant fixtures ($n = 3$) were subjected to *in vivo* bioluminescence as previously described [34]. All procedures were performed at the University of Michigan Small Animal Imaging Resource Facility (http://www.med.umich.edu/msair/). This procedure was performed at 1, 3, 7, 10, 14, 21, 28, and 35 ± 1 days or until gene expression was no longer present. The imaging method utilized the CCD IVISTM system with a 50-mm lens (Xenogen Corp., Alameda, CA, USA). All images were analyzed using the LivingImage software package (Xenogen Corp.). Animals were given intraperitoneal injections of luciferin (Promega Corp., Madison, WI, USA) at a dose of 150 mg/kg in sterile saline. The animals then were anesthetized using a 1.75% isoflurane/air mixture. Dorsal images were taken for 10 min in length at 15–25 min postinjection. To localize the signal, color images of the photon emissions were superimposed on gray-scale images of the animals and signals were quantified in RLU (Fig. 1C). The animals were kept warm and monitored until consciousness resumed.

Biopsy harvest and histological preparation

The animals were sacrificed by CO_2 euthanasia at 14 ($n = 5$ animals; 10 implants per group) and 28 ($n = 10$ animals; 20 implants per group) days following surgery. The other animals (total of 14 from day 3 to 10) were also assessed. Block biopsies were harvested and immediately fixed and stored in 10% formalin for 7 days and then transferred to 70% alcohol. Blocks subsequently were dehydrated in step gradients of alcohol and were infiltrated and embedded in methyl methacrylate by routine histological methods. Each block contained one implant and the orientation of the sections was sagittal along the length of the fixture. Serial sections approximately 50 μm in thickness were made by using a diamond wire saw, representing the midportion of each implant site (Well Diamond Wire Saws, Inc., Norcross, GA, USA). Each section was attached to a plastic slide (Wasatch Histo Consultants, Inc., Winnemucca, NV, USA), ground to approximately 25 μm using an EXAKT Micro Grinder 400 (Exakt Medical Instruments, Inc., Oklahoma City, OK, USA), and polished to an optical finish [31]. One section per implant site was left unstained for fluorescence and SEM analysis,

and the remaining section was stained using basic fuschin/toluidine blue for histomorphometric analysis.

After histological preparation, slides were coded and examined by two blinded examiners. Slides were excluded from the study if they displayed processing errors that would inhibit valid measurements, including tangential sections or large artifacts. Any implants that exhibited fibrous encapsulation due to failed osseointegration (4) were also excluded. Examiners were unaware of the treatment performed and had to arrive at a consensus on any exclusions.

Scanning electron microscopy

After histological measurement of the slides, samples were analyzed using SEM to determine the nature of the new bone-to-implant contact. Slides were reduced in size to fit properly on the mounting. Samples were mounted with graphite and left to dry overnight. Slides then were coated with gold and visualized at 30×, 100×, 300×, and 1000× using an Amray 1000B scanning electron microscope (Amray, Bedford, MA, USA).

Histometric analysis

The histologic analysis served to evaluate the spatial and temporal sequence of osteogenesis during dental implant osseointegration. Histomorphometric analyses were performed using a Nikon E800 microscope (Nikon, Inc., Melville, NY, USA) fitted with a video camera and Image Pro Plus analysis software (Media Cybernetics, Silver Spring, MD, USA). Two calibrated examiners evaluated the slides (C.D. and Q.J.). Analysis of standard parameters of osteogenesis were performed as previously described [35-37] and comparisons between each group were done with Student's *t* tests using statistic software SPSS 12.0 (SPSS, Inc., Chicago, IL, USA). The parameters analyzed were as follows:

1. Percentage defect fill: the percentage of new bone in the defect area, i.e., the new bone area in the defect divided by the defect area.
2. New bone implant contact (BIC): the percentage of new BIC including the entire perimeter of the implant, i.e., the length of new bone contacting the implant divided by the length of the implant in millimeters.
3. New coronal bone fill: total area of new bone coronal to the base defect area in square millimeters, not to exceed the total width of the defect.

Acknowledgments

This study was funded by NIH/NIDCR Grants DE 13397 to W.V.G. and DE 13386 to R.T.F., a Delta Dental Fund to C.D., and The American Academy of Implant Dentistry Research Foundation to C.D. The authors appreciate Cathy Mayton for her histological expertise, Daniel Hall for his assistance with the in vivo bioluminescence, Chris Edwards for his assistance with the SEM, Mike Setter for surgical assistance, and Chris Jung for the illustrations. We also thank Steven Goldstein and the University of Michigan Bone Core for their helpful discussions and histological assistance with our pilot studies (Grant P30-AR46024). The imaging studies were supported in part by a grant awarded to Brian Ross at the Center of Molecular Imaging at the University of Michigan (NIH/NCI Grant R24 CA83099).

References

1. Schropp L, Wenzel A, Kostopoulos L, Karring T. Bone healing and soft tissue contour changes following single-tooth extraction: a clinical and radiographic 12-month prospective study. Int. J. Periodont. Restor. Dent 2003;23:313–323.
2. Hammerle CH, Glauser R. Clinical evaluation of dental implant treatment. Periodontology 2000 2004;34:230–239. [PubMed: 14717865]
3. Giannobile WV. Periodontal tissue engineering by growth factors. Bone 1996;19:23S–37S. [PubMed: 8830996]

4. Reddi AH. Role of morphogenetic proteins in skeletal tissue engineering and regeneration. Nat. Biotechnol 1998;16:247–252. [PubMed: 9528003]
5. Hogan BL. Bone morphogenetic proteins: multifunctional regulators of vertebrate development. Genes Dev 1996;10:1580–1594. [PubMed: 8682290]
6. Reddi AH. BMPs: actions in flesh and bone. Nat. Med 1997;3:837–839. [PubMed: 9256271]
7. Aberg T, Wozney J, Thesleff I. Expression patterns of bone morphogenetic proteins (Bmps) in the developing mouse tooth suggest roles in morphogenesis and cell differentiation. Dev. Dyn 1997;210:383–396. [PubMed: 9415424]
8. Amar S, et al. Markers of bone and cementum formation accumulate in tissues regenerated in periodontal defects treated with expanded polytetrafluoroethylene membranes. J. Periodontal Res 1997;32:148–158. [PubMed: 9085226]
9. Thomadakis G, Ramoshebi LN, Crooks J, Rueger DC, Ripamonti U. Immunolocalization of bone morphogenetic protein-2 and -3 and osteogenic protein-1 during murine tooth root morphogenesis and in other craniofacial structures. Eur. J. Oral Sci 1999;107:368–377. [PubMed: 10515202]
10. Giannobile WV, et al. Recombinant human osteogenic protein-1 (OP-1) stimulates periodontal wound healing in class III furcation defects. J. Periodontol 1998;69:129–137. [PubMed: 9526911]
11. Rutherford RB, Sampath TK, Rueger DC, Taylor TD. Use of bovine osteogenic protein to promote rapid osseointegration of endosseous dental implants. Int. J. Oral Maxillofacial Implants 1992;7:297–301.
12. van den Bergh JP, ten Bruggenkate CM, Groeneveld HH, Burger EH, Tuinzing DB. Recombinant human bone morphogenetic protein-7 in maxillary sinus floor elevation surgery in 3 patients compared to autogenous bone grafts: a clinical pilot study. J. Clin. Periodontol 2000;27:627–636. [PubMed: 10983596]
13. Doll B, Sfeir C, Winn S, Huard J, Hollinger J. Critical aspects of tissue-engineered therapy for bone regeneration. Crit. Rev. Eukaryotic Gene Expression 2001;11:173–198.
14. Alden TD, et al. The use of bone morphogenetic protein gene therapy in craniofacial bone repair. J. Craniofacial Surg 2000;11:24–30.
15. Jin QM, Anusaksathien O, Webb SA, Rutherford RB, Giannobile WV. Gene therapy of bone morphogenetic protein for periodontal tissue engineering. J. Periodontol 2003;74:202–213. [PubMed: 12666709]
16. Jin Q, Anusaksathien O, Webb SA, Printz MA, Giannobile WV. Engineering of tooth-supporting structures by delivery of PDGF gene therapy vectors. Mol. Ther 2004;9:519–526. [PubMed: 15093182]
17. Doukas J, et al. Matrix immobilization enhances the tissue repair activity of growth factor gene therapy vectors. Hum. Gene Ther 2001;12:783–798. [PubMed: 11339895]
18. Linkhart TA, Mohan S, Baylink DJ. Growth factors for bone growth and repair: IGF, TGF beta and BMP. Bone 1996;19:1S–12S. [PubMed: 8830994]
19. Paralkar VM, Nandedkar AK, Pointer RH, Kleinman HK, Reddi AH. Interaction of osteogenin, a heparin binding bone morphogenetic protein, with type IV collagen. J. Biol. Chem 1990;265:17281–17284. [PubMed: 2211625]
20. Cook SD, et al. The effect of recombinant human osteogenic protein-1 on healing of large segmental bone defects. J. Bone Joint Surg. Am 1994;76:827–838. [PubMed: 8200889]
21. Krebsbach PH, Gu K, Franceschi RT, Rutherford RB. Gene therapy-directed osteogenesis: BMP-7-transduced human fibroblasts form bone in vivo. Hum. Gene Ther 2000;11:1201–1210. [PubMed: 10834621]
22. Yang Y, et al. Cellular immunity to viral antigens limits E1-deleted adenoviruses for gene therapy. Proc. Natl. Acad. Sci. USA 1994;91:4407–4411. [PubMed: 8183921]
23. Lieberman JR, et al. Regional gene therapy with a BMP-2-producing murine stromal cell line induces heterotopic and orthotopic bone formation in rodents. J. Orthop. Res 1998;16:330–339. [PubMed: 9671928]
24. Rutherford RB, et al. Bone morphogenetic protein-transduced human fibroblasts convert to osteoblasts and form bone in vivo. Tissue Eng 2002;8:441–452. [PubMed: 12167230]

25. Nussenbaum B, Rutherford RB, Teknos TN, Dornfeld KJ, Krebsbach PH. Ex vivo gene therapy for skeletal regeneration in cranial defects compromised by postoperative radiotherapy. Hum. Gene Ther 2003;14:1107–1115. [PubMed: 12885349]
26. Franceschi RT, Wang D, Krebsbach PH, Rutherford RB. Gene therapy for bone formation: in vitro and in vivo osteogenic activity of an adenovirus expressing BMP7. J. Cell. Biochem 2000;78:476–486. [PubMed: 10861845]
27. Jin QM, Zhao M, Economides AN, Somerman MJ, Giannobile WV. Noggin gene delivery inhibits cementoblast-induced mineralization. Connect. Tissue Res 2004;45:50–59. [PubMed: 15203940]
28. Musgrave DS, et al. Adenovirus-mediated direct gene therapy with bone morphogenetic protein-2 produces bone. Bone 1999;24:541–547. [PubMed: 10375195]
29. Okubo Y, et al. The time course study of osteoinduction by bone morphogenetic protein-2 via adenoviral vector. Life Sci 2001;70:325–336. [PubMed: 12005265]
30. Alden TD, Varady P, Kallmes DF, Jane JA Jr. Helm GA. Bone morphogenetic protein gene therapy. Spine 2002;27:S87–S93. [PubMed: 12205425]
31. Chen Y, et al. Gene therapy for new bone formation using adeno-associated viral bone morphogenetic protein-2 vectors. Gene Ther 2003;10:1345–1353. [PubMed: 12883531]
32. Luk KD, et al. Adeno-associated virus-mediated bone morphogenetic protein-4 gene therapy for in vivo bone formation. Biochem. Biophys. Res. Commun 2003;308:636–645. [PubMed: 12914798]
33. Morohashi T, et al. Defects in mandibular bone area, enamel iron content and dentine formation following gastrectomy in rats. Arch. Oral Biol 2002;47:499–504. [PubMed: 12102767]
34. Kalikin LM, et al. In vivo visualization of metastatic prostate cancer and quantitation of disease progression in immunocompromised mice. Cancer Biol. Ther 2003;2:656–660. [PubMed: 14688471]
35. McCracken M, Lemons JE, Zinn K. Analysis of Ti-6Al-4V implants placed with fibroblast growth factor 1 in rat tibiae. Int. J. Oral Maxillofacial Implants 2001;16:495–502.
36. Nevins ML, Karimbux NY, Weber HP, Giannobile WV, Fiorellini JP. Wound healing around endosseous implants in experimental diabetes. Int. J. Oral Maxillofacial Implants 1998;13:620–629.
37. Becker W, et al. A comparison of ePTFE membranes alone or in combination with platelet-derived growth factors and insulin-like growth factor-I or demineralized freeze-dried bone in promoting bone formation around immediate extraction socket implants. J. Periodontol 1992;63:929–940. [PubMed: 1453308]

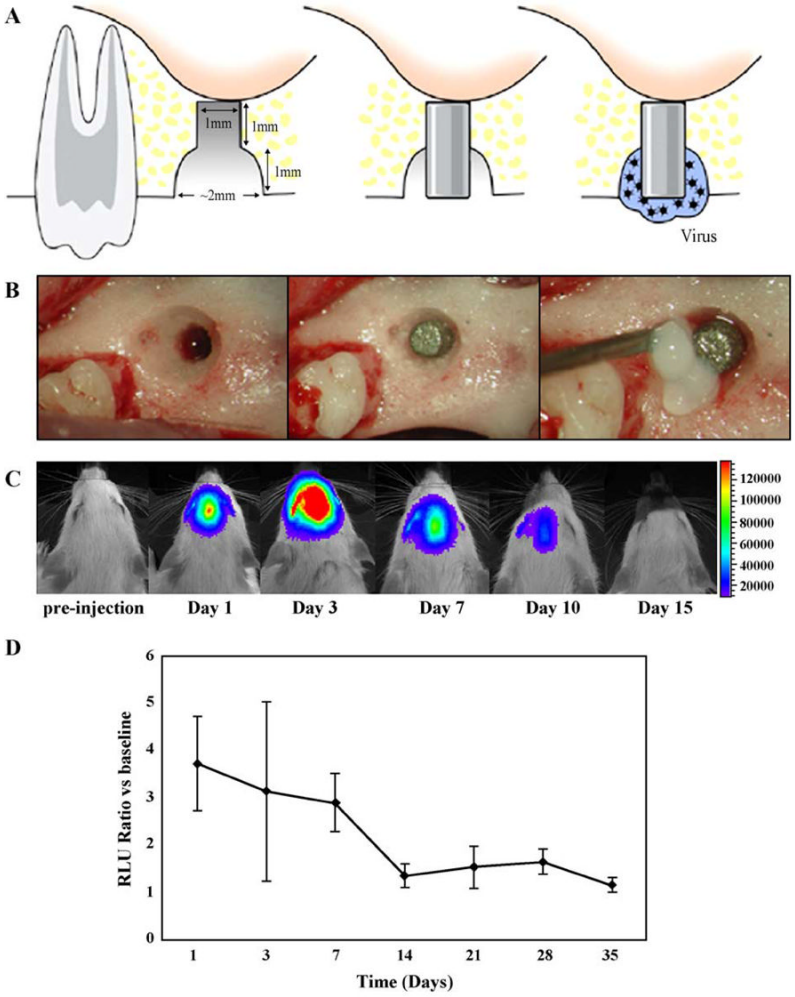

Fig. 1.

Gene targeting model to evaluate dental implant osseointegration. (A) Dental implant osteotomy defect model for gene delivery. “Well-type” osteotomy defects were created that measured 1 mm in depth and 2 mm coronally (left). The titanium dental implant was press fit into position (middle), followed by the delivery of the 2.6% collagen matrix containing either Ad/BMP-7 or Ad/Luc (right). (B) High-magnification images from the surgical operation corresponding to (A) taken at 10× magnification including defect creation (left), dental implant placement (middle), and gene delivery (right). (C) *In vivo* bioluminescence of gene targeting. *In vivo* bioluminescence images of a luciferase-treated rat. Dorsal images were taken for 10 min at 15 to 25 min postinjection. To localize the signal, color images of the photon emissions were superimposed on gray-scale images of the animals and signals were quantified in relative light units (RLU). All images were analyzed using the LivingImage software. Distribution of gene delivery is shown beginning at day 1 with the peak expression at day 4. In this case, transgene expression was sustained at measurable levels for 10 days. Photon emissions were measured in RLU. (D) Means ± SEM of the ratios of the RLU versus preinjection baseline controls of Ad/Luc delivered to the implant osteotomy defects.

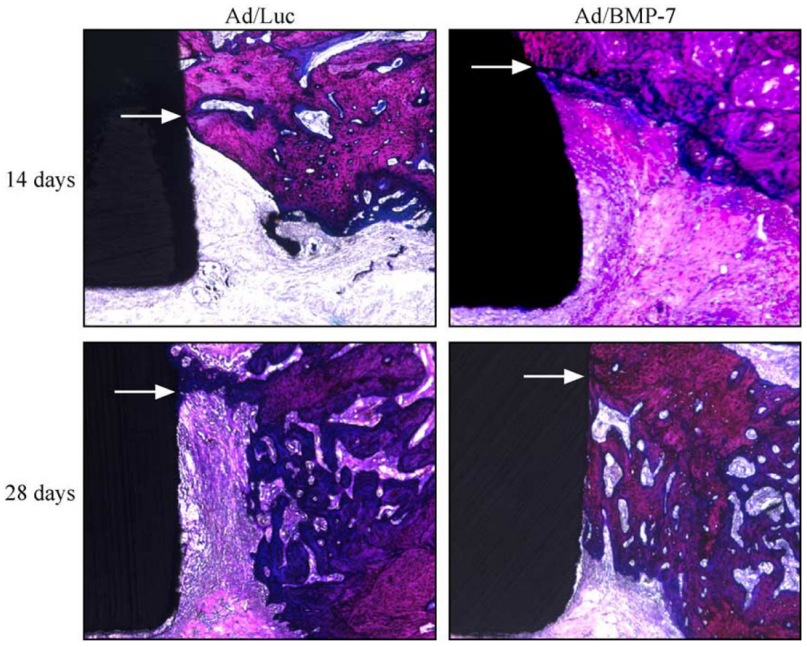

Fig. 2.

Ad/BMP-7 stimulates alveolar bone engineering at dental implant sites. Block biopsies were taken at 3, 7, 10, 14, and 28 days post-gene delivery and implant placement for descriptive histology and histomorphometric analysis. At 14 days post-surgery and gene delivery, early bone formation was seen along the defect borders. Several of the Ad/BMP-7-treated defects displayed tissue consistent with early osteoid formation throughout the defect area. The Ad/Luc group exhibited normal bone healing, with most specimens showing minimal bone formation at the defect borders. Arrows point to the base of the osteotomy defects and the implant fixture is positioned inferiorly, shown in the sagittal orientation. Sections were stained with basic fuschin/toluidine blue histological staining at 4× original magnification.

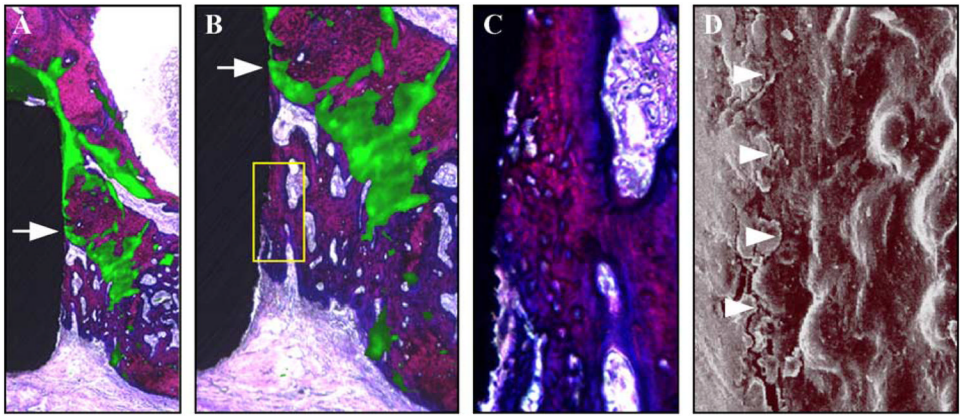

Fig. 3.

BMP-7 gene delivery stimulates dental implant osseointegration. (A) Histological staining overlaid with calcein bone fluorochrome to demarcate new and old bone from Ad/BMP-7-treated defect at 28 days at low power (1× magnification). (B) The defect border is clearly evident, and the new bone is bridging the defect and the implant surface (2× original magnification). (C) New bone-to-implant contact can be noted along the implant surface from the break-out box noted in (B). (D) Scanning electron microscopic image demonstrating intimate contact of new alveolar bone with the dental implant surface (1000× original magnification). Arrow points to the base of the osteotomy defects, while arrowheads point to the new bone-to-implant contact.

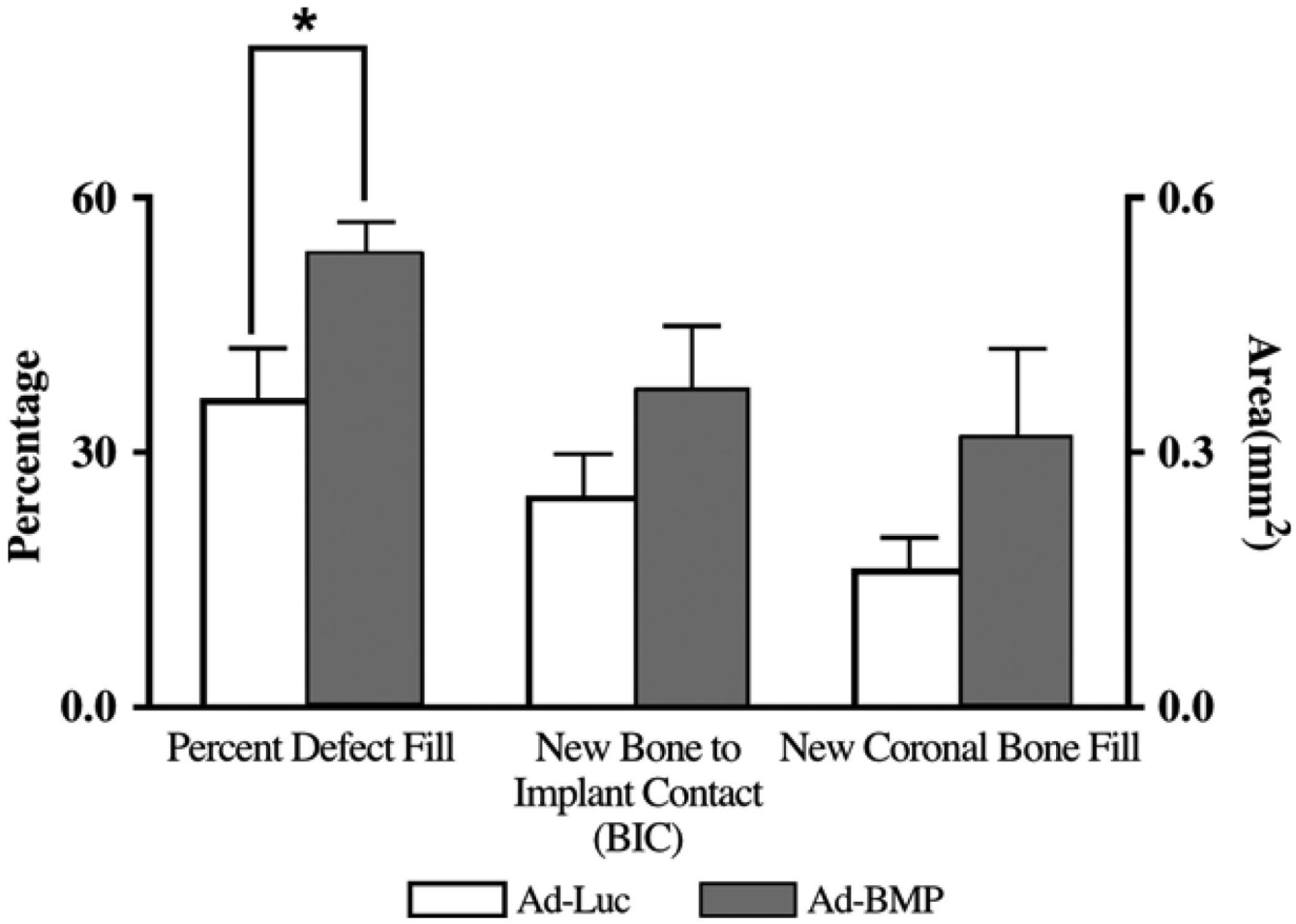

Fig. 4.

BMP-7-mediated gene delivery accelerates dental implant osseointegration. The Ad/BMP treatment significantly increased the percentage bone defect fill in the defects by 50% ($P < 0.05$) compared to the Ad/Luc-treated group at 28 days post-gene delivery. The Ad/BMP-7 treatment also tended to enhance both coronal new bone formation (>2-fold compared to the Ad/Luc group) and new bone-to-implant contact (by 50% compared to Ad/Luc). Statistical analysis was performed using Student's *t* test via software SPSS 12.0 (SPSS, Inc.) ($n = 16$ animals).